Energy Conversion and Management 165 (2018) 236–243

Contents lists available at ScienceDirect

Energy Conversion and Management

journal homepage: www.elsevier.com/locate/enconman

Simulation study on the degradation process of photovoltaic modules

Chao Huang[a,b], Long Wang[c,*]

[a] School of Automation, Guangdong University of Technology, Guangzhou 510006, China
[b] Department of Systems Engineering and Engineering Management, City University of Hong Kong, Kowloon, Hong Kong Special Administrative Region
[c] School of Computer and Communication Engineering, University of Science and Technology Beijing (USTB), Beijing 100083, China

ARTICLE INFO

Keywords:
Aging factors
Performance degradation
Photovoltaic modules
Simulation

ABSTRACT

Degradation decreases photovoltaic power delivery capacity over time. Studies on photovoltaic degradation are usually based on accelerated tests or filed tests which are time-consuming and require much effort. This paper investigates the degradation process of photovoltaic modules by simulation studies. A circuit-based model is employed to describe photovoltaic characteristics to environmental conditions and to the aging factors of photovoltaic modules. Analysis of each aging factor shows that the decrease of short-circuit current, the main reason of power loss, is mainly caused by optical degradation. The decay of fill factor mainly due to degradation of parasitic resistances worsens the power output. The statistical analysis of photovoltaic characteristic parameters based on a great number of photovoltaic modules with the same technology indicates that the degradation process can be very complicated depending on the degradation patterns of aging factors. Generally, the power loss tends to increase and the mismatch among photovoltaic modules becomes more remarkable through the time.

1. Introduction

Photovoltaic (PV) module is considered as the most reliable component in a PV system, and its life time is expected to be more than 20 years. Degradation, however, decreases the PV power delivery capacity over time [1]. A thorough understanding of PV module degradation is required to make better use of PV module during its life time.

Studies on PV degradation often investigate the degradation modes, mechanisms, and degradation rates. The reported degradation modes include cell cracks, hot spots, glass soiling, ethylene vinyl acetate (EVA) browning, delamination, coating oxidation, etc., for crystalline silicon PV modules operated over 20 years in Italy [2]. These degradation models were also observed in PV modules of other technologies and exposed to various climates. In [3], Malvoni et al. studied the long-term performance loss of a 960 kWp PV system in the Mediterranean climate and concluded that the PV system demonstrated good performance compared to other plants located in the same climate. Kichou et al. [4] investigated the degradation modes and degradation rates of thin-film PV modules exposed to relatively dry and sunny climate in Spain. Bouraiou et al. [5] investigated the impacts of high temperature and the other climatic factors in the Saharan environment on the performance of PV modules installed in the desert region in south of Algeria. Chandel et al. [6] presented the performance degradation of mono-crystalline-silicon PV generator after 28 years of exposure at a western Himalayan in India, and the main defects observed in PV modules were encapsulant discoloration, delamination, oxidation of front grid fingers, and glass breakages. In [7], Jordan et al. concluded that hot spot was the most important degradation mode for crystalline modules installed in the last 10 years while the glass breakage and absorber corrosion dominated the degradation models for thin-film PV technologies. It was also concluded that PV modules exposed to hot and humid climates show considerably higher degradations modes than those in desert and moderate climates. These degradation modes decrease the light approaching the semiconductor junction and worsen the internal electrical properties of PV modules leading to the loss in power production. In [8], the long-term performance degradation rates of 12 PV systems with different technologies including monocrystalline silicon, multicrystalline silicon, amorphous silicon (a-Si), cadmium telluride (CdTe), copper indium gallium diselenide (CIGS) were investigated and the degradation rates varied significantly among these technologies. In [9], nearly 2000 degradation rates were reviewed showing a median annual performance degradation rate of 0.5% and that location and PV technology were most influential factors determining degradation rate. Accelerated tests and outdoor tests which are time-consuming and require substantial efforts are the most frequently applied approaches to study degradation of PV modules. It took hundreds of hours to run the thermal cycling stress test to estimate the degradation rate of multi-

* Corresponding author.
E-mail address: lwang@ustb.edu.cn (L. Wang).

https://doi.org/10.1016/j.enconman.2018.03.056
Received 23 October 2017; Received in revised form 15 March 2018; Accepted 19 March 2018
0196-8904/

Nomenclature

I_{pv}	light-generated current
R_s	series resistance
R_p	shunt resistance
I_0	diode reverse saturation current
a	diode ideality factor
V_T	thermal voltage
N_s	cells in series of a PV module
k	Boltzmann constant
q	electron charge
T	PV cell temperature
I	terminal current of a PV module
V	terminal voltage of a PV module
I_{sc}	short-circuit current
V_{oc}	open-circuit voltage
G	solar irradiation
$I_{pv,ref}$	I_{pv} at reference conditions
T_{ref}	T at reference conditions
G_{ref}	G at reference conditions
k_I	temperature coefficient of I_{sc}
k_V	temperature coefficient of V_{oc}
τ	transmittance of a PV module
P_{max}	maximal power
FF	fill factor
t	the index of time
$\tau(t)$	τ at time t
$R_s(t)$	R_s at time t
$R_p(t)$	R_p at time t
$I_{pv}(t)$	I_{pv} at time t
$V(t)$	V at time t
$I(t)$	I at time t
μ_0	initial mean value
σ_0	initial standard deviation
$\mu(t)$	mean value at time t
$\sigma(t)$	standard deviation at time t
A	variation rate of μ
B	variation rate of σ

crystalline silicon PV modules under well controlled conditions in [10]. The outdoor experiments could last from several years to more than 20 years. Hence, a simple and fast approach to investigate the degradation of PV performance over time regardless of the PV technology and the installed location is of great value.

Indeed, a PV plant usually consists of dozens or hundreds of PV modules. Degradation process can provoke mismatch among PV modules. It is interesting that the standard deviation of peak power of 42 crystalline silicon PV modules after 12-year operation in Southern Europe slightly decreased compared to initial value in [11]. However, the standard deviation of peak power of 191 PV modules after 11 years of field exposure to a cool and coastal environment in California, USA, showed a greatly increase [12]. This mismatch of peak power among PV modules may cause a variety of problems to the PV system [13], such as the presence of multiple local maxima of the PV plant which can mislead the maximal power point tracking (MPPT) algorithm failing to extract the most power from the array. A better understanding of the distribution of power output of PV modules will benefit the PV management system, and help improve the prediction accuracy of PV power production over time.

Simulation provides an easy and fast approach to study the characteristics of PV modules [14]. Such studies are often used to investigate response of PV modules to environmental factors [15] and to develop MPPT algorithms [16]. Nowadays, simulation is also applied to analyze the influence of degradation on PV module characteristics. Doumane et al. [17] investigated power loss of a PV module over years based on an equivalent electrical circuit by tuning the circuit parameters associated with the aging of PV modules, and this work was conducted in a deterministic manner. However, a PV plant is composed of dozens or hundreds of PV modules and the aging process of each module could be quite different. A PV array is usually composed of PV modules with the same technology. Hence, it will be of great value to investigate the degradation process considering a great number of PV modules with the same technology that the electrical properties of PV modules are considered independent and identically distributed in statistics.

The aim of this paper is to investigate the degradation process of PV module performance by simulation considering a great number of PV modules with the same technology. The investigation will concentrate on the statistical analysis on the degradation of PV characteristic parameters for the considered PV modules through the time. To this end, a circuit-based model is developed to describe the general electrical characteristics of PV modules in Section 2. In Section 3, the effects of each aging factor on PV module performance are analyzed relying on the circuit-based model. This is followed by simulation study on the degradation process of a great number of PV modules over a long period under assumptions that the considered PV modules with the same technology are independent and their electrical properties follow the same probability distribution. Results show that the degradation process can be very complicated depending on the aging patterns of related factors. Generally, the mismatch among PV modules become more remarkable through the time. The conclusion and perspective are provided in Section 4.

2. Modeling of photovoltaic module characteristics

A PV cell is a semiconductor device fabricated in a thin wafer or layer that converts solar power to electricity. And a PV module usually consists of dozens of PV cells in series. The equivalent circuit of a PV module in Fig. 1 shows a good compromise between complexity and accuracy in modeling PV characteristics, and it is widely used to express the electrical characteristics of a PV module. The light-generated current I_{pv} is proportional to the effective irradiance and is affected by cell temperature. The diode expresses the exponential *I-V* characteristics of a PV module. The equivalent series resistance R_s and equivalent shunt resistance R_p present the power loss due to the parasitic resistances in practical PV modules. The equivalent series resistance R_s includes resistances from metallic contacts, cell solder bonds, cell-interconnection bars, junction-box terminations, and inner diode. The shunt resistance R_p represents any parallel high-conductivity shunts across the solar cell p-n junction or on the cell edges. In general case, the value of R_p is much higher than that of R_s, while in ideal case the value of R_p is infinite and the value of R_s is zero.

According to Kirchhoff laws, the *I-V* characteristics depicted in Fig. 1 can be mathematically expressed as:

$$I = I_{pv} - I_0\left[\exp\left(\frac{V + R_s I}{aV_T}\right) - 1\right] - \frac{V + R_s I}{R_p} \quad (1)$$

where I_{pv} is the light-generated current; I_0 is the diode reverse

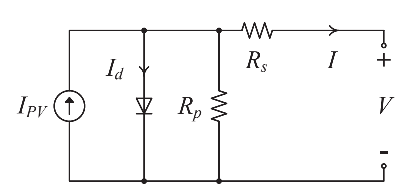

Fig. 1. The schematic of PV module equivalent circuit.

saturation current; a is the diode ideality factor; R_s and R_p are the series resistance and the shunt resistance, respectively; $V_T = N_s kT/q$ is the thermal voltage of PV module with N_s cells in series; k is the Boltzmann constant ($1.3806503 \times 10^{-23}$ J/K); q is the electron charge ($1.60217646 \times 10^{-19}$ C); and T (K) is the cell temperature.

In (1), five model parameters, the light-generated current I_{pv}, the diode reverse saturation current I_0, the series resistance R_s, the shunt resistance R_p, and the diode ideality factor a, are required to define the *I-V* characteristics. I_{pv} depends on the incident irradiation and cell temperature and is strongly influenced by the optical degradation of PV module; I_0 depends on the cell temperature; R_s and R_p depend on the aging of module; a is a constant.

The dependence of light-generated current I_{pv} on incident solar irradiation G and cell temperature T is expressed as [18]:

$$I_{pv} = [I_{pv,ref} + k_I(T - T_{ref})]\frac{G}{G_{ref}}\tau \tag{2}$$

where $I_{pv,ref}$ is light-generated current at the reference conditions, usually the standard test conditions (STC) of irradiation of 1000 W/m^2, cell temperature of 25 °C, and air mass of 1.5; k_I (A/K) is the temperature coefficient of short-circuit current; T and T_{ref} are the actual and reference cell temperature; G and G_{ref} are the actual irradiation and reference irradiation; the dimensionless variable τ measures the transmittance of PV module, which decreases over time due to optical degradation, and the relative initial value is set as 1.

The dependence of diode reverse saturation current I_0 on cell temperature T is formulated as [19]:

$$I_0 = \frac{I_{sc,ref} + k_I(T - T_{ref})}{\exp\left[\frac{V_{oc,ref} + k_V(T - T_{ref})}{aV_T}\right] - 1} \tag{3}$$

where k_V (V/K) is the open-circuit voltage temperature coefficient; $I_{sc,ref}$ and $V_{oc,ref}$ are the short-circuit current and open-circuit voltage at the reference conditions, respectively.

The *I-V* characteristics depending on environmental conditions and the status of PV module are described by (1)–(3) making it possible to study the effects of aging factors on PV characteristics.

3. Analysis and discussion

In this section the effects of aging factors on PV performance will firstly be analyzed. This is followed by the investigation on the degradation process of a great number of PV modules with the same technology.

3.1. Analysis on effects of aging factors on photovoltaic module performance

Due to outdoor exposure to irradiance, temperature, humidity, wind, and physical stress like snow and hail, power delivery capacity of a PV module decreases over time. The commonly observed degradation modes include material corrosion, delamination, discoloration of encapsulant over cells, and breakage or cracks of modules. These degradation modes affect the PV characteristics in three ways: decreasing transmittance τ, increasing series resistance R_s, and decreasing shunt resistance R_p [20,21]. In this section, the effects of each factor related to aging on PV characteristic parameters, including short-circuit current I_{sc}, open-circuit voltage V_{oc}, maximal power P_{max}, and fill factor ($FF = P_{max}/I_{sc}V_{oc}$) are quantitively analyzed. The FF describes the ideality of a PV module, and a lower value of FF than ideal is caused by the parasitic resistances and non-ideal diode.

The effects of aging factors on PV characteristics parameters are illustrated by numerical case studies based on KC200GT PV module. The multi-crystal KC200GT PV module with nominal power of 200 W is manufactured by Kyocera, and it is widely used in grid-connected PV systems. The nominal characteristic parameters of KC200GT PV module

Table 1
Nominal specifications of KC200GT PV module under STC.

Parameter	Value
Maximum power P_{max}	200 W
Maximum power voltage V_{mpp}	26.3 V
Maximum power current I_{mpp}	7.61 A
Open circuit voltage V_{oc}	32.9 V
Short circuit current I_{sc}	8.21 A
Temperature coefficient of V_{oc}	−0.123 V/°C
Temperature coefficient of I_{sc}	3.18×10^{-3} A/°C
Diode ideal factor a	1.3
Series resistance R_s	0.221 Ω
Shunt resistance R_p	415.4 Ω

at STC and corresponding equivalent circuit model parameters are given in Table 1. The investigation on effects of each aging factor on PV characteristic parameters is conducted by tuning the value of corresponding aging factor and observing the characteristic parameters with the simulation model under STC.

3.1.1. Effects of decreasing transmittance

Many factors, such as corrosion of glass, discoloration of encapsulant, and degradation of anti-reflective coating can cause optical degradation. Fig. 2 depicts the effects of a decreasing transmittance τ, from initial value of 1 to 0.75, and to 0.5, on *I-V* characteristics of KC200GT PV module under STC. The maximal power points (MPP) for various transmittances are also shown in the figure.

It is observable that the decreasing transmittance τ reduces both I_{sc} and V_{oc}. The PV characteristic parameters for various transmittances are provided in Table 2. When the transmittance decreases from 1 to 0.75 and to 0.5, both I_{sc} and P_{max} are reduced by about 25% and 50%. The FF and V_{oc} show little variation compared to the change of I_{sc}. The effect of decreasing transmittance τ on power loss is almost linear mainly from the loss of I_{sc}; therefore, a small decrease in transmittance can be detrimental to the PV power output.

3.1.2. Effects of parasitic resistances

Although PV cells and modules are designed to minimize the series resistance losses, the series resistance R_s increases gradually under outdoor exposure. Metallic corrosion which reduces the conductivity contributes to the increase of R_s. An increase in the shunt paths across the p-n junction may decrease the value of shunt resistance R_p. The effects of parasitic resistances on PV performance have been studied in [22], however, the extremely cases where large deviation of parasitic resistances from initial values are not presented. The effects of increasing R_s and decreasing R_p on *I-V* curve under STC are depicted in Fig. 3.

The increasing R_s has no effect on V_{oc}, but reduces I_{sc}. The

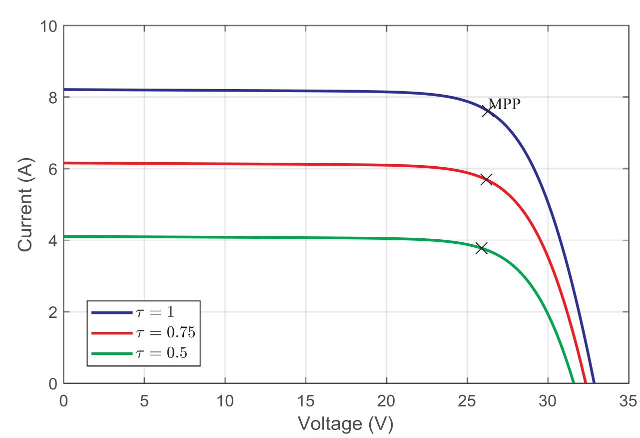

Fig. 2. Effects of decreasing transmittance on *I-V* characteristics at reference conditions.

Table 2
Effects of decreasing transmittance on PV characteristic parameters.

τ	I_{sc} (A)	V_{oc} (V)	P_{max} (W)	*FF*
1	8.21	32.8	200.1	0.743
0.75	6.16	32.3	149.1	0.750
0.5	4.10	31.6	97.7	0.754

Table 3
Effects of increasing series resistance on PV characteristic parameters.

R_s (Ω)	I_{sc} (A)	V_{oc} (V)	P_{max} (W)	*FF*
0.221	8.21	32.8	200.1	0.743
2.21	8.17	32.8	103.3	0.386
4.42	6.73	32.8	57.4	0.260

Table 4
Effects of decreasing shunt resistance on PV characteristic parameters.

R_p (Ω)	I_{sc} (A)	V_{oc} (V)	P_{max} (W)	*FF*
415.4	8.21	32.8	200.1	0.743
41.54	8.17	32.7	185.2	0.693
4.514	7.80	29.3	66.5	0.291

decreasing R_p reduces both I_{sc} and V_{oc}. Tables 3 and 4 present I_{sc}, V_{oc}, P_{max}, and *FF* for different values of R_s and R_p, respectively. When R_s is increased by 10 times from 0.221 Ω to 2.21 Ω, I_{sc} show little variation while P_{max} and *FF* are reduced by about 50%. At even higher value of R_s (4.42 Ω, 20 times of the initial value), the reduction of I_{sc} is significant. When the R_p decreases from 415.4 Ω to 41.54 Ω, the variation of PV performance is small. However, at very low value of R_p, 4.154 Ω, the situation gets much worse that the *FF* thereby the P_{max} decreases dramatically.

With the above analysis, it becomes clear that the decrease of I_{sc} is mainly caused by decreasing τ, while the increasing R_s and decreasing R_p result in decreasing *FF*. The mixed effects lead to the loss of P_{max}.

The numerical case study illustrates the way that the aging factors affect PV module characteristic parameters and the magnitudes of the effects by simulation studies. The methodology can be extended to other PV technologies and applied to real PV modules exposed to outdoor conditions.

3.2. Analysis on the degradation process of photovoltaic modules

In the field, the aging factors occur continuously as the year progresses. To study the combined effects of aging factors on PV characteristics, the electrical characteristics of a PV module in (1)–(3) are written as (4)–(6) by considering the progress of aging factors through the time:

$$I(t) = I_{pv}(t) - I_0\left\{\exp\left[\frac{V(t)+R_s(t)I(t)}{aV_T}\right]-1\right\} - \frac{V(t)+R_s(t)I(t)}{R_p(t)} \tag{4}$$

$$I_{pv}(t) = I_{pv,ref}[1+k_I(T-T_{ref})]\frac{G}{G_{ref}}\tau(t) \tag{5}$$

$$I_0 = \frac{I_{sc,ref}+k_I(T-T_{ref})}{\exp\left[\frac{V_{oc,ref}+k_V(T-T_{ref})}{aV_T}\right]-1} \tag{6}$$

Here, the transmittance $\tau(t)$, the series resistance $R_s(t)$, and shunt resistance $R_p(t)$ are time dependent variables presenting the aging process of materials over time, thereby the *I-V* characteristics are not only a function of irradiation *G* and cell temperature *T*, but also a function of time *t*.

If the degradation patterns of each aging factor in (4)–(6) are available, it is possible to characterize the degradation pattern of PV characteristic parameters. There is, however, little information on the degradation pattern of these aging factors. Warranty on PV module power output is usually in the range of 20–25 years that the power output will be more than 80% of its initial rated power after the guaranteed years of operation. Thus, degradation of PV module is a gradual and steady process. In [23], it is assumed that the power output of PV modules with the same technology follows a Gaussian distribution, and the mean power of PV modules decreases linearly. Inspired by the idea, it is assumed that each aging factor including the transmittance τ, the series resistance R_s, and shunt resistance R_p follows a Gaussian distribution as in (7) for a large population of PV modules with the same technology.

$$p(y) = \frac{1}{\sqrt{2\pi}\sigma}\exp\left[-\frac{1}{2}\left(\frac{y-\mu}{\sigma}\right)^2\right] \tag{7}$$

where *y* refers to the aging factor τ, R_s, or R_p, μ is its mean value, and σ is its standard deviation. It is not clear on the dependence of these three aging factors to each other or on the variation of their yearly degradation rates and standard deviations over time. In this study, the following assumptions are also considered: (i) aging factors are independent; (ii) the mean value and standard deviation of each aging factor varies linearly as in (8) and (9).

$$\mu(t) = \mu_0(1+At) \tag{8}$$

$$\sigma(t) = \sigma_0(1+Bt) \tag{9}$$

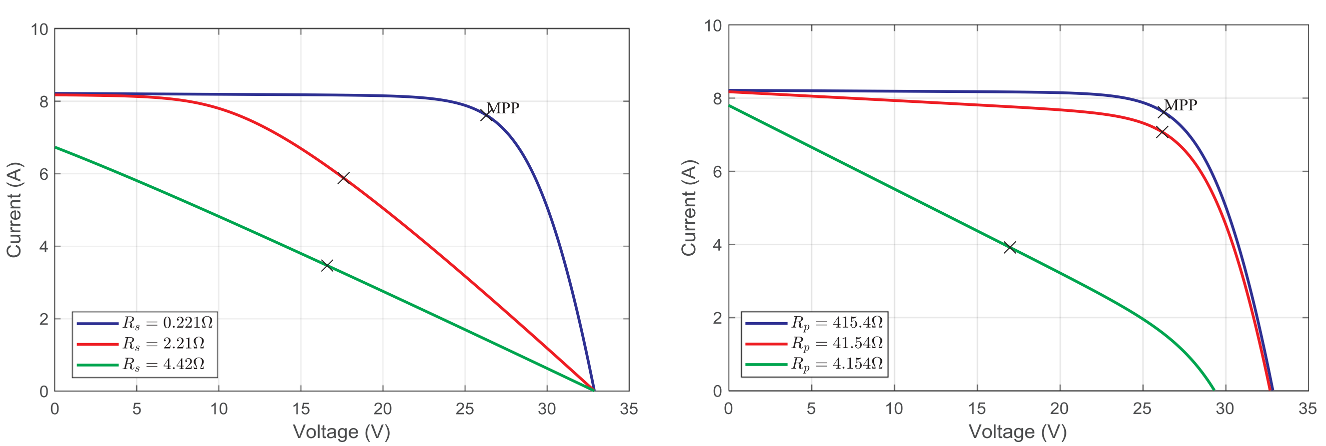

(a) Effects of series resistance R_s (b) Effects of shunt resistance R_p

Fig. 3. Effects of parasitic resistances on *I-V* curve under STC.

where μ_0 and σ_0 are the initial mean value and standard deviation at $t = 0$; A and B are the variation rate in percentage of the mean value and standard deviation, respectively; t is the time in years. $\lambda_0 = \sigma_0/\mu_0$ is defined to describe σ_0 in percentage of μ_0.

The technique of Monte Carlo (MC) simulation [24], which relies on repeated random sampling to obtain numerical results, is widely used to derive the probability distribution of an unknown random variable. To obtain the distributions of PV characteristic parameters through the time, following steps are deployed with Monte Carlo simulation technique: (i) determine the mean value and standard deviation at year t with (8) and (9) for each aging factor; (ii) randomly sample the values of each aging factor according to its distribution defined in (7); (iii) construct *I-V* characteristics with (4)–(6) under given environmental conditions of G and T; (iv) repeat steps (ii) and (iii) for N times. With these steps, N *I-V* curves can be obtained at year t considering the random degradation process of each aging factor. In this study, $N = 5000$ is considered and the distributions of PV characteristic parameters at year t are derived with the 5000 *I-V* curves.

The degradation rate of PV modules highly depends on the PV technology and the climate. Hence, the choice of degradation model parameters in (7)–(9) including λ_0, A, and B can be in a wide range. The following case studies are used to illustrate the application of the developed simulation model into the analysis of the degradation process of PV modules. To make a comprehensive comparison of aging patterns on PV characteristic parameters, different values of λ_0, A, and B by enumerating possible values and utilizing degradation data derived from long-term field operation are considered, while the other model parameters including R_s and R_p at year $t = 0$, k_I, k_V, and a are based on specifications of KC200GT PV module.

3.2.1. Case study by enumerating degradation data

To simply the analysis, the standard deviation of each aging factor is supposed to be constant over time, namely $B = 0$. The values of μ_0, λ_0, and A for each aging factor are given in Table 5. Analysis in Section 3.1 shows that the effect of transmittance τ on power is almost linear, while the effects of parasitic resistances are totally non-linear which could be disastrous for PV power output in extremely cases. Thus, two levels of standard deviation of shunt resistance are compared to better understand the impacts of parasitic resistances. Larger is the standard deviation of parasitic resistances, more possible is to observe the extremely cases (the observed value is far from the initial value) of degradation of parasitic resistances.

The Monte-Carlo simulation technique described above is applied to obtain the distribution of PV characteristic parameters through the time. Fig. 4 shows the probability density distribution (PDF) of maximal power before and after 20 years (common warranty of PV module) simulated operation at two levels of standard deviation of shunt resistance. The results are obtained under the nominal operating cell temperature (NOCT) conditions, irradiation of 800 W/m^2 and ambient temperature of 20 °C (47 °C cell temperature provided by datasheet), which are considered closer to the actual operating conditions.

After 20 years, the maximal power decreases obviously, and the mean of maximal power shows little deviation between two levels of standard deviation of shunt resistance. The maximal power drops from 142.2 W to 113.8 W, and from 142.0 W to 112.1 W for the lower and the higher level of standard deviation of shunt resistance, respectively. The corresponding annual power loss rates are 0.999% and 1.05%, respectively. However, the distributions of maximal power are quite different. At the beginning, the distributions of maximal power under two cases fit well normal distribution. At the year of 20, in the case of smaller standard deviation of shunt resistance, the distribution of maximal power still matches well with normal distribution shown in Fig. 4(a); in the case of larger standard deviation of shunt resistance, the distribution of maximal power is far from normal distribution shown in Fig. 4(b). The probability of PV modules that their power productions are more than 80% of initial rated power (113.6 W under NOCT) is 99.88% with smaller standard deviation of shunt resistance, however, the number is reduced to 96.92% as the standard deviation of shunt resistance is doubled.

To better explain the effects of two levels of standard deviation of shunt resistance on PV characteristics, the mean value (μ) and standard deviation (σ) of each characteristic parameter through the time is shown in Fig. 5. These characteristic parameters include maximal power P_{max}, short-circuit current I_{sc}, open-circuit voltage V_{oc}, and fill factor FF, and the observation period is expended to 30 years.

The mean of P_{max} and I_{sc} shows little difference between two levels of variance of R_p. The larger standard deviation of R_p lowers the mean of V_{oc} and FF. The decay of I_{sc} contributes the main part of power loss which is worsened by the decrease of FF.

The standard deviation of each characteristic parameter over time shows great difference between two levels of standard deviation of R_p. In the case of smaller standard deviation of R_p, the standard deviation of each characteristic parameter almost keeps constant at the first 25 years. At the year of 30, however, the standard deviation starts to increase due to more observations of the extremely low value of R_p. Extremely low R_p could greatly reduce the values of V_{oc} and FF thereby the P_{max}. In the case of larger standard deviation of R_p, the standard deviations of P_{max}, V_{oc}, and FF tend to increase from the beginning of simulation. The impact of R_p on I_{sc} is very weak except at extremely low value of R_p, thus the standard deviation of I_{sc} varies little during the first 10 years.

From above analysis, the degradation process of PV characteristic parameters can be significantly different depending on the degradation patterns of aging factors. Generally, the loss of power tends to increase and the mismatch among PV modules becomes more remarkable through the time.

3.2.2. Case study with 11-year field data in California

Studies in [12] investigated the outdoor performance of 191 mono-Si PV modules exposed to a cool and coastal environment for 11 years in California, USA. The comparison of PV module parameters before and after 11-year operation and the average annual change rates are given in Table 6. In this case study, the change rates of I_{sc}, R_s, and R_p derived from long-term field data are used to define corresponding parameters in the simulation model as in Table 7.

The statistics of PV characteristic parameters before simulated aging process, after 10-year simulated operation, and after 20-year simulated operation under NOCT are provided in Table 8. It is observable that the average annual degradation rates as well as the standard deviations of P_{max}, I_{sc}, V_{oc}, and FF increase through the time. The decay of I_{sc} contributes most to the loss of P_{max}.

The distributions of P_{max} through the time are depicted in Fig. 6. After 20 years, there are 73.94% PV modules that their power outputs are more than 80% of initial rated power. However, it is observable that PV modules with extremely low P_{max} are frequently observed after 20 years. This is due to the decreasing mean value but increasing standard deviation of R_p that the possibility to observe very low values of R_p greatly increases. The average annual degradation rate of P_{max} in this case study is lower than the ones in Section 3.2.1. However, the mismatch among PV modules is much more remarkable, and this will cause difficulties in PV system management such as maximum power point tracking.

In this section, the model to simulate the degradation process of PV

Table 5
Value of μ_0, A, and λ_0 for each aging factor.

	μ_0	A (%)	λ_0 (%)	
τ	1	−0.5	2	
R_s	0.221 Ω	2	20	
R_p	415.4 Ω	−2	15	30

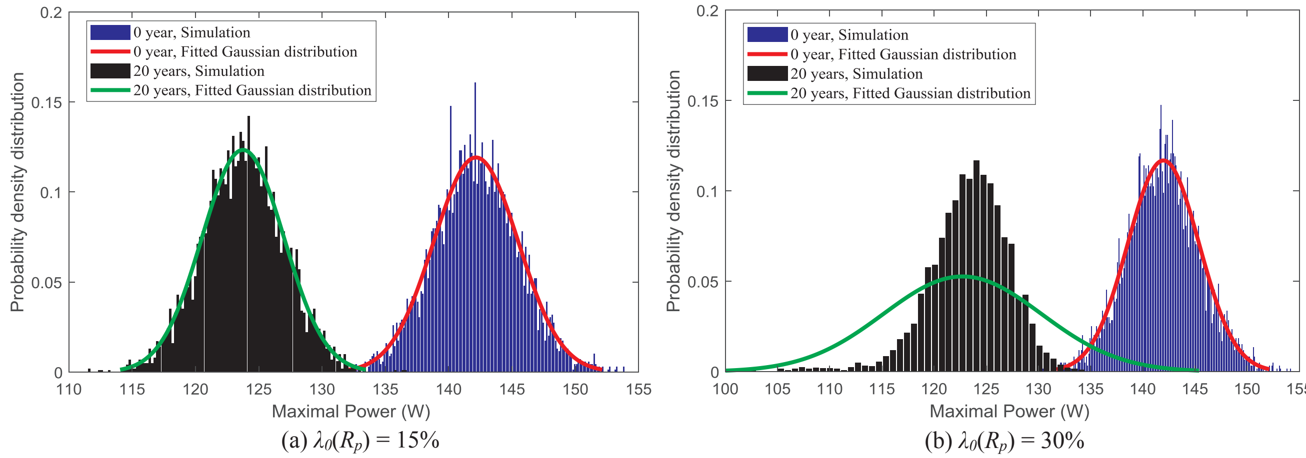

Fig. 4. PDF of maximal power before and after 20 years simulated operation at NOCT.

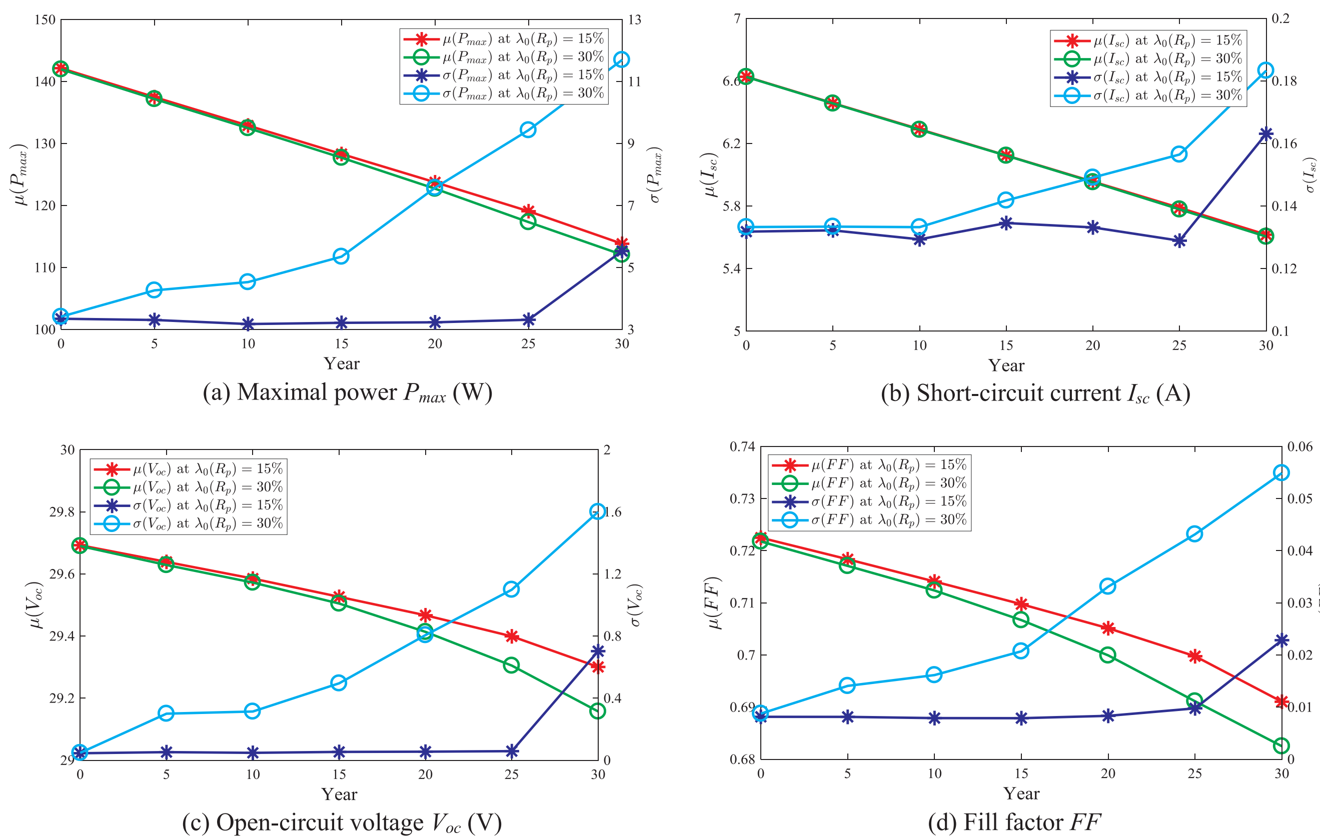

Fig. 5. Mean (μ) and standard deviation (σ) of characteristic parameters over time.

Table 6
Comparison of PV module parameters before and after 11-year field operation [12].

Parameter	Initial			Final			Change/year	
	μ	σ	σ/μ (%)	μ	σ	σ/μ (%)	μ (%)	σ (%)
P_{max} (W)	39.88	0.849	2.13	38.13	1.67	4.38	−0.40	8.79
I_{sc} (A)	3.29	0.044	1.34	3.08	0.12	3.90	−0.58	15.70
V_{oc} (V)	18.19	0.131	0.72	18.15	0.108	0.60	−0.02	−1.60
R_s (Ω)	0.347	0.115	33.14	0.384	0.184	47.92	0.97	5.45
R_p (Ω)	171	39.2	22.92	115	48.7	42.35	−2.98	2.20

Table 7
Simulation parameters based on field degradation rates.

	μ_0	A (%)	λ_0 (%)	B (%)
τ	1	−0.58	1.34	15.70
R_s	0.221 Ω	0.97	33.14	5.45
R_p	415.4 Ω	−2.98	22.92	2.20

modules are developed. As the degradation patterns and the correlations of the aging factors are not clear, assumptions that the aging factors are independent, follow Gaussian distribution, and vary linearly through the time are considered to simplify the study. However, the simulation method can also be applied if the correlations among aging factors are unveiled by further research or the aging factors are demonstrated to follow other distributions such as inverse Gaussian distribution.

Table 8
PV characteristic parameters through the time.

Parameter	0-year		10-year		Change/year μ (%)	20-year		Change/year μ (%)
	μ	σ	μ	σ		μ	σ	
P_{max} (W)	141.98	3.31	131.42	7.40	−0.68	119.03	13.84	−0.81
I_{sc} (A)	6.62	0.09	6.23	0.23	−0.54	5.84	0.39	−0.59
V_{oc} (V)	29.69	0.03	29.54	0.37	−0.05	29.28	1.37	−0.07
FF	0.72	0.01	0.71	0.03	−0.10	0.69	0.06	−0.19

4. Conclusion and perspective

In this paper, a simulation method is presented to study the degradation process of PV modules. This method relies on a circuit-based model of PV electrical characteristics. The model relates the PV characteristics to the environmental conditions (irradiation and temperature) and to the aging factors of PV modules.

Study on the effects of each aging factor on PV characteristics shows that the decrease of short-circuit current, the main reason of power loss, is mainly caused by optical degradation of PV modules, while the decay of fill factor mainly due to parasitic resistances degradation worsens the power output. PV module designers can benefit from this analysis in minimizing the influence of degradation on PV performance.

Much effort has been made on the investigation of statistical analysis of PV characteristic parameters over time under assumptions on the degradation pattern of each aging factor. In the case studies, different scenarios are considered to investigate the degradation process of PV modules. Numerical results show that the degradation process of PV characteristic parameters can be very complicated depending on the aging patterns of related factors. Generally, the power loss of PV modules tends to increase and the mismatch among PV modules becomes more remarkable through the time. These case studies are based on KC200GT PV modules by enumerating possible degradation rates of aging factors and utilizing degradation data derived from long-term field operation. Practically, the aging patterns highly depend on PV technology and climates that PV modules expose to. The proposed simulation method can be extended to analyze the degradation process of other PV technologies and operating conditions by replacing corresponding model parameters such as Rs, Rp, A, B, and λ0 for a prospective PV technology under a given climate.

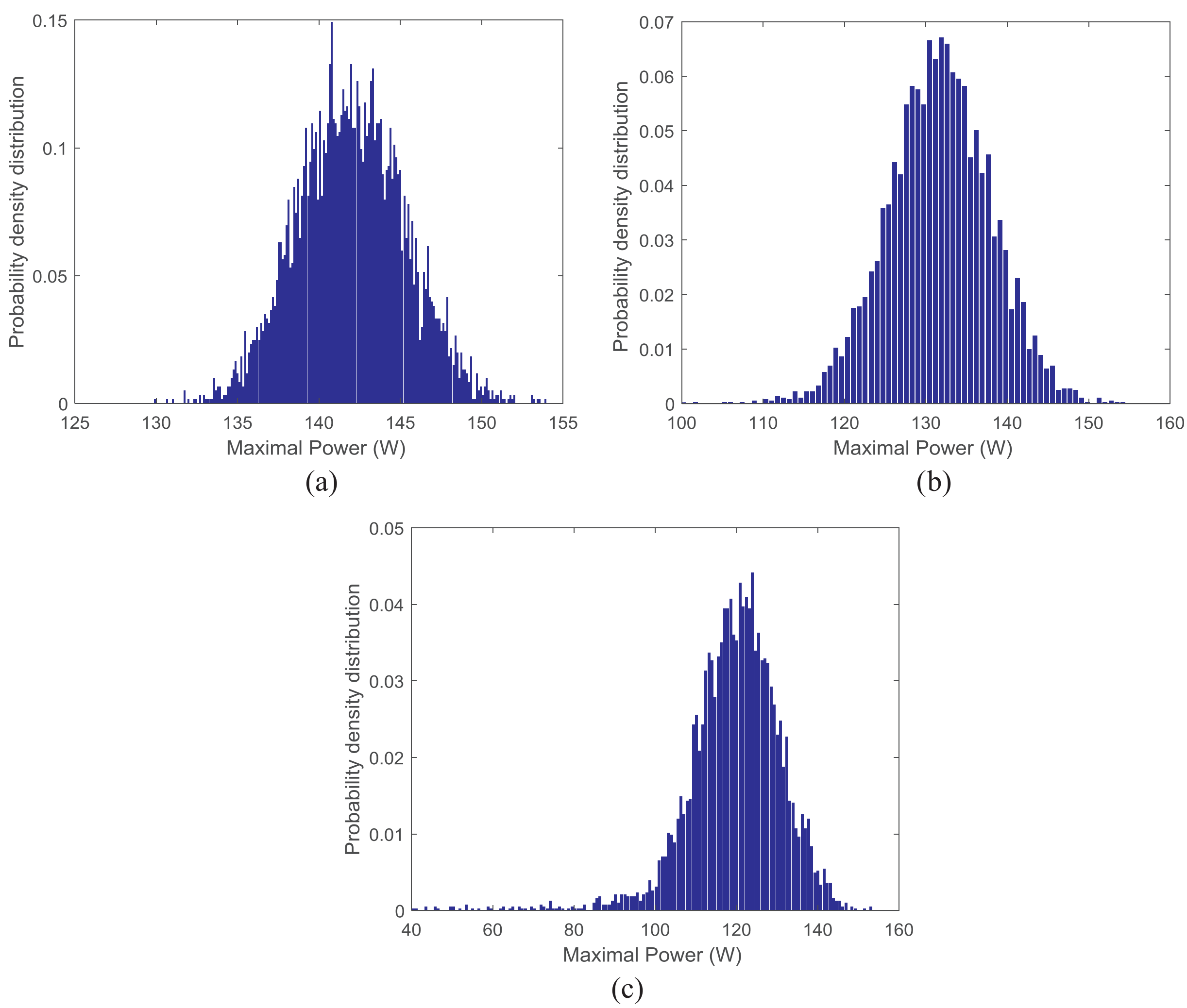

Fig. 6. Distributions of P_{max} through the time, (a) 0-year; (b) 10-year; (c) 20-year.

Acknowledgement

This work was supported by the Fundamental Research Funds for the Central Universities under Grant 06500078.

References

[1] Jordan DC, Deline C, Kurtz SR, Kimball GM, Anderson M. Robust PV degradation methodology and application. IEEE J Photovoltaics 2018;8:525–31.

[2] Polverini D, Field M, Dunlop E, Zaaiman W. Polycrystalline silicon PV modules performance and degradation over 20 years. Progress Photovolt.: Res. Appl. 2013; p. 1004–15.

[3] Malvoni M, Leggieri A, Maggiotto G, Congedo P, De Giorgi M. Long term performance, losses and efficiency analysis of a 960 kWp photovoltaic system in the Mediterranean climate. Energy Convers Manage 2017;145:169–81.

[4] Kichou S, Abaslioglu E, Silvestre S, Nofuentes G, Torres-Ramírez M, Chouder A. Study of degradation and evaluation of model parameters of micromorph silicon photovoltaic modules under outdoor long term exposure in Jaén, Spain. Energy Convers Manage 2016;120:109–19.

[5] Bouraiou A, Hamouda M, Chaker A, Mostefaoui M, Lachtar S, Sadok M, et al. Analysis and evaluation of the impact of climatic conditions on the photovoltaic modules performance in the desert environment. Energy Convers Manage 2015;106:1345–55.

[6] Chandel S, Naik MN, Sharma V, Chandel R. Degradation analysis of 28 year field exposed mono-c-Si photovoltaic modules of a direct coupled solar water pumping system in western Himalayan region of India. Renewable Energy 2015;78:193–202.

[7] Jordan DC, Silverman TJ, Wohlgemuth JH, Kurtz SR, VanSant KT. Photovoltaic failure and degradation modes. Progress Photovolt. April 2017; 25: p. 318–26.

[8] Makrides G, Zinsser B, Schubert M, Georghiou GE. Performance loss rate of twelve photovoltaic technologies under field conditions using statistical techniques. Sol Energy 2014;103:28–42.

[9] Jordan DC, Kurtz SR. Photovoltaic degradation rates-an analytical review. Progress Photovolt. January 2013;21:12–29.

[10] Park N, Jeong J, Han C. Estimation of the degradation rate of multi-crystalline silicon photovoltaic module under thermal cycling stress. Microelectron Reliab August 2014;54:1562–6.

[11] Sánchez-Friera P, Piliougine M, Peláez J, Carretero J, Sidrach de Cardona M. Analysis of degradation mechanisms of crystalline silicon PV modules after 12 years of operation in Southern Europe. Prog Photovoltaics Res Appl 2011;19:658–66.

[12] Reis AM, Coleman NT, Marshall MW, Lehman PA, Chamberlin CE. Comparison of PV module performance before and after 11-years of field exposure. In: Conference record of the twenty-ninth IEEE photovoltaic specialists conference 2002; 2002. p. 1432–35.

[13] Olalla C, Deline C, Maksimovic D. Performance of mismatched PV systems with submodule integrated converters. IEEE J Photovoltaics 2014;4:396–404.

[14] Chin VJ, Salam Z, Ishaque K. An accurate modelling of the two-diode model of PV module using a hybrid solution based on differential evolution. Energy Convers Manage 2016;124:42–50.

[15] Wang L, Huang C. A novel Elite Opposition-based Jaya algorithm for parameter estimation of photovoltaic cell models. Optik-Int J Light Electron Opt 2018;155:351–6.

[16] Huang C, Wang L, Yeung RS-C, Zhang Z, Chung H, Bensoussan A. A prediction model guided Jaya algorithm for the PV system maximum power point tracking. IEEE Trans Sustainable Energy 2017.

[17] Doumane R, Balistrou M, Logerais P, Riou O, Durastanti J, Charki A. A circuit-based approach to simulate the characteristics of a silicon photovoltaic module with aging. J Sol Energy Eng 2015;137:021020.

[18] Mahmoud Y, Xiao W, Zeineldin HH. A simple approach to modeling and simulation of photovoltaic modules. IEEE Trans Sustainable Energy Jan 2012;3:185–6.

[19] Villalva MG, Gazoli JR, Ruppert Filho E. Comprehensive approach to modeling and simulation of photovoltaic arrays. IEEE Trans Power Electron 2009;24:1198–208.

[20] Miller DC, Annigoni E, Ballion A, Bokria JG, Bruckman LS, Burns DM, et al. Degradation in PV encapsulation transmittance: an interlaboratory study towards a climate-specific test. In: Photovoltaic Specialist Conference (PVSC), 2015 IEEE 42nd; 2015. p. 1–6.

[21] Kahoul N, Houabes M, Sadok M. Assessing the early degradation of photovoltaic modules performance in the Saharan region. Energy Convers Manage 2014;82:320–6.

[22] van Dyk EE, Meyer EL. Analysis of the effect of parasitic resistances on the performance of photovoltaic modules. Renewable Energy March 2004;29:333–44.

[23] Vazquez M, Rey-Stolle I. Photovoltaic module reliability model based on field degradation studies. Progress Photovolt. August 2008;16:419–33.

[24] Rubinstein RY, Kroese DP. Simulation and the Monte Carlo method, vol. 10. John Wiley & Sons; 2016.